

УДК 641.528

## Исследование напряженных состояний конструкций в процессе ползучести с целью оценки наибольшего напряжения

Федорова Л.А., канд. техн. наук, проф. Малявко Д.П.,

Елисеев А.М. [Elianto992@gmail.com](mailto:Elianto992@gmail.com)

Университет ИТМО

Институт холода и биотехнологий

921002, Санкт-Петербург, ул. Ломоносова, 9

*Представленные решения дают анализ напряженного состояния рассмотренных конструкций, согласно которому определяются максимальные напряжения в материале конструкций для  $n=1$  (состояние линейной упругости) и для  $n=\infty$  (решение в случае идеальной пластичности). Все решения приведены для различных геометрических параметров конструкций, различных граничных условий и нескольких значений  $m$  ( $m=1/n$ ). Результаты вычислений показаны графически. В соответствии с графиками определяются значения относительного коэффициента концентрации напряжения  $F_m$ . Если коэффициент  $F_m$  известен, то максимальные напряжения в конструкции в состоянии ползучести нетрудно оценить (на основе линейно-упругого анализа) в зависимости от нагрузки и геометрических характеристик этой конструкции.*

*Показано, что если распределение напряжений известно для случая линейной упругости ( $n=1$ ), то скорость изменения напряжений (и, в особенности, максимального напряжения) в зависимости от  $n$  можно определить, по существу, подобно решению задачи о линейно-упругих температурных напряжениях, так как «температурные» деформации выражаются в большей степени в изменении формы, чем в изменении объема.*

*Ключевые слова:* ползучесть, изгибающий момент, радиальное и окружное напряжения, деформация, граничное условие.

---

## Investigation of stress state for estimating the greatest stress in structures subject to creep

*The solutions to be represented give analysis of stress state of the structures considered. According to this analysis the greatest stresses in the structures for  $n=1$  (linear-elastic structures) and  $n=\infty$  (the perfectly plastic solution) are determined. All the solutions are given for different parameters of the structures, different boundary conditions and several values of  $m$  ( $m=1/n$ ). The results are shown graphically. According to the graphs relative stress concentration factor  $F_m$  can be determined. As  $F_m$  is known, the greatest stress in a structure subject to creep may be estimated without too much difficulty (by linear-elastic analysis) in terms of the applied load and the geometrical parameters of the structure.*

*It is shown, that if the stress distribution is known in the linear case ( $n=1$ ), the rate of change of the stresses (and in particular of the greatest stress) with  $n$  may be determined from, essentially, a linear-elastic thermal stress problem as the “thermal” strains consist of changes in shape rather than changes in volume.*

*Keywords:* creep, bending moment, radial and circumferential stresses, strain, boundary condition.

---

The structures considered [1] are shown schematically in Table 1.

All the usual assumption of linear-elastic small deflection theory are used [5]; thus we learn nothing, for example, about local stress concentration effects in the regions where plates

join thicker plates (structure E) or rigid foundations (structure D). Nor do we learn anything about plates with membrane action.

Thus while it may seem paradoxical that acute, local, stress concentration effects have been ignored, it seems clear that the study, in so far as it leads to empirical general conclusions, may be of some use in tackling problems of local stress concentration factors.

In Fig. 1 the relative stress concentration factor  $F_m$  [1] is plotted against the material parameter  $m$ , which is the reciprocal of the exponent  $n$  [1]:

$$m = \frac{1}{n}.$$

The factor  $F_m$  is defined as on the following equation [1]:

$$F_r = \frac{\text{Greatest stress in structure for material } n = r}{\text{Greatest stress in structure for material } n = 1},$$

But with an obvious change of subscript.

For most of the structures solutions were obtained, in addition to those for  $n=1$  and  $n=\infty$  ( $m=1$  and  $m=0$ , respectively) for  $m=0.1; 0.2; 0.4; 0.6; \text{ and } 0.8$

Table 1 gives for each structure the value of the greatest stress,  $\bar{\tau}_{max}$  in terms of the load and geometrical parameters for the case  $n=1$ . Use of this expression in conjunction with the appropriate graph in Fig. 1 gives the value of  $\bar{\tau}_{max}$  for any load and value of the exponent  $n$ .

Further details of the methods of solution for the various structures are represented (they were not given in paper [1] because their inclusion would have made it too long)

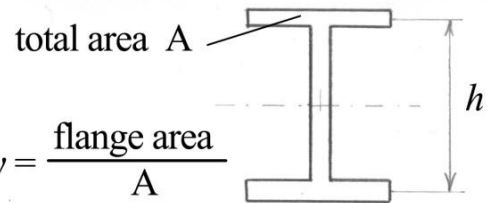
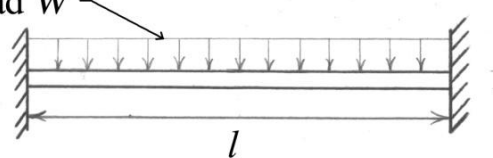
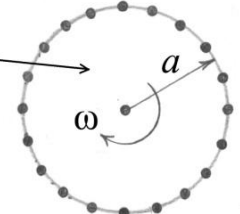
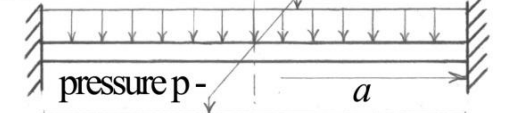
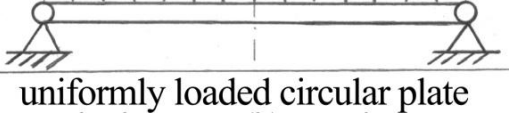
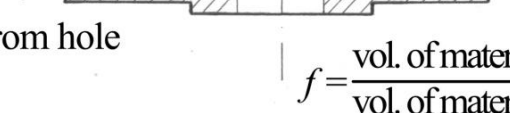
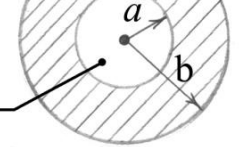
A	 <p>total area A</p> <p>flange area</p> <p><math>v = \frac{\text{flange area}}{A}</math></p> <p>axis of bending - moment M</p> <p>h</p>	$\sigma_{\max, n=1} = \frac{M}{Ah} \cdot \frac{6}{2\nu+1}$
I - section in pure bending		
B	 <p>total load W</p> <p>h</p> <p>l</p> <p>cross section as in A above</p>	$\sigma_{\max, n=1} = \frac{Wl}{Ah} \cdot \frac{1}{2\nu+1}$
uniformly loaded beam with clamped ends		
C	 <p>mass density <math>\rho</math></p> <p><math>\omega</math></p> <p>a</p> <p>total uniformly distributed edge mass = <math>\beta</math> * mass of disc</p>	$\bar{\sigma}_{\max, n=1} = \frac{\rho a^2 \omega^2}{g} \left( \frac{7}{16} + \frac{\beta}{2} \right)$
rotating parallel - sided disc		
D	 <p>(a)</p> <p>pressure p -</p> <p>a</p> <p>h</p>	$(a) \bar{\sigma}_{\max, n=1} = p \frac{a^2}{h^2} \cdot \frac{3\sqrt{3}}{6}$
	 <p>(b)</p> <p>h</p>	$(b) \bar{\sigma}_{\max, n=1} = p \frac{a^2}{h^2} \cdot \frac{21}{16}$
uniformly loaded circular plate (a) clamped edge (b) simply supported edge		
E	 <p>stress p remote from hole</p> <p>a b</p> <p><math>f = \frac{\text{vol. of material added}}{\text{vol. of material cut out}}</math></p>	$\sigma_{\max, n=1} = p \frac{2}{1 + \frac{3}{4} \frac{f a^2}{b^2}}$
symmetrical stretched sheet with hole and ring reinforcement		
F	 <p>closed ends</p> <p>internal pressure p</p> <p>a b</p>	$\bar{\sigma}_{\max, n=1} = p \frac{b^2 \sqrt{3}}{b^2 - a^2}$
thick - walled tube under internal pressure		

Table 1.

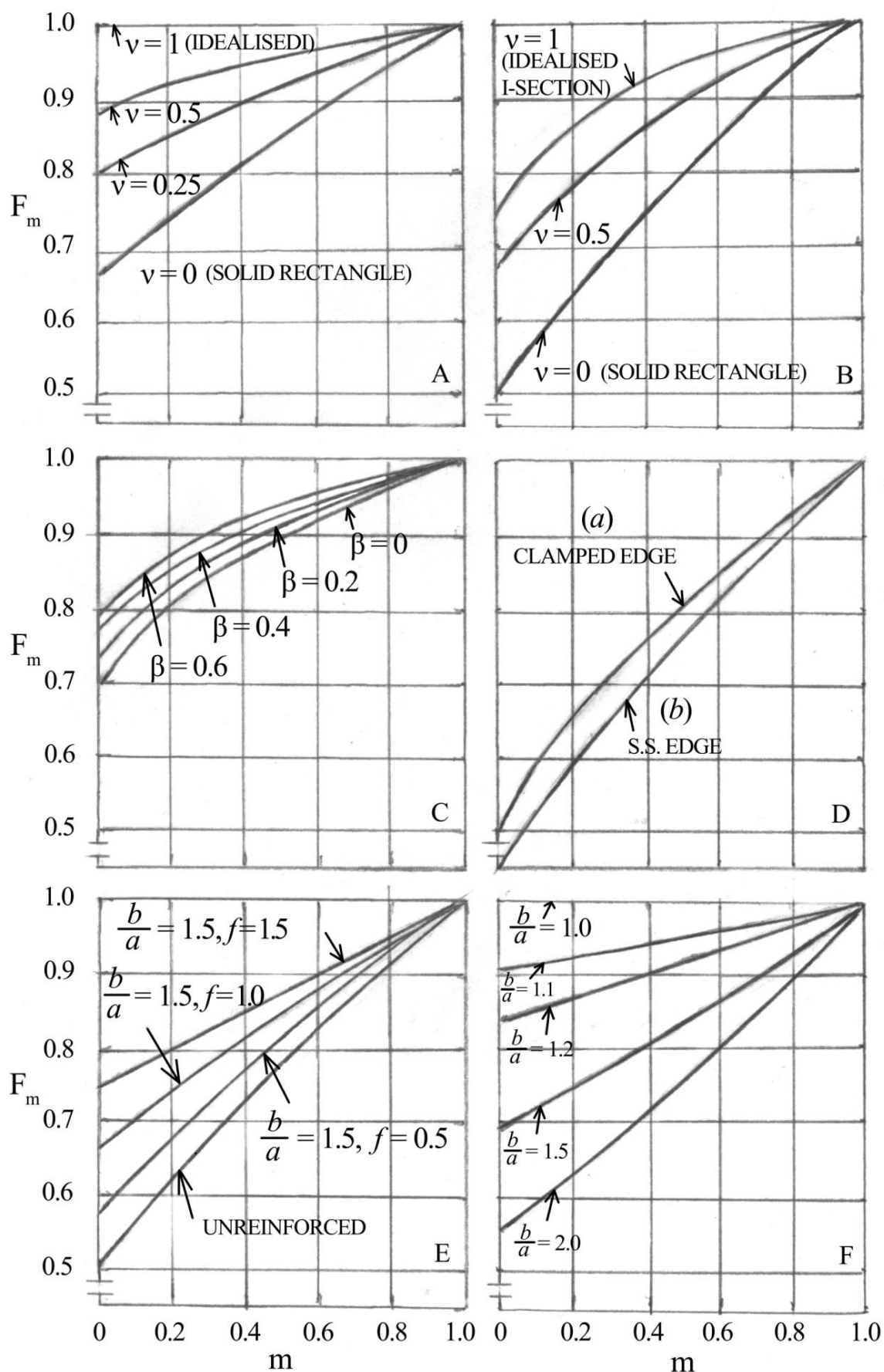


Fig.1 Results for structures shown in Table 1

### Details of the various solutions.

#### A. I – section in pure bending.

This is a very simple problem. By symmetry the neutral axis is at the centre of the section. As “plane sections remain plane” it is a straightforward matter to express the strain rate at any distance  $y$  from the neutral axis in terms of  $y$ , the rate of change of curvature of the section, and the material constants [7]. Appropriate integration gives the bending moment, and a little algebra puts the results in the desired form.

#### B. Uniformly loaded beam with clamped ends.

The origin was taken at the centre, and the ends of the beam were regarded as “floating boundaries”.

By statics the bending moment is of the form

$$M = M_0 - \frac{Wx^2}{2}$$

The rate of change of curvature,  $\dot{k}$  is related to the bending moment by a law [3]

$$\dot{k} = DM^n,$$

In which  $D$  depends on the cross-section shape and size and the material constant  $B$ . Thus for any finite value of  $n$ ,  $\dot{k}$  may be determined as a function of  $x$ . Integration of  $\dot{k}$  with respect to  $x$  gives the rate of change of slope. Which is zero by symmetry at  $x=0$ . Integrating graphically to  $x=l$  for which

$$\int_0^l \dot{k} dx = 0$$

Gives the value of  $x$  at the end of the beam: this is used in the first equation to give the fixed-end moment  $M$ , which is readily expressed in terms of the total distributed load and the length of the beam. For the case  $n \rightarrow \infty$  conventional perfectly plastic analysis is used. Use of the results of A, above, enables the results to be presented in the form of Fig. 1.

#### C. Rotating parallel sided disc.

The equilibrium equation at radius  $r$  is

$$\frac{d\tau_r}{dr} = \frac{\tau_\theta - \tau_r}{r} - \alpha_r, \dots \dots \dots (1)$$

Where  $\tau_r$  and  $\tau_\theta$  are radial and circumferential stress, respectively,

$$\alpha = \frac{\rho\omega^2}{g} \dots \dots \dots (2)$$

And  $\rho$  and  $\omega$  as defined in Fig. 1. The strain rate compatibility equation is

$$\frac{d\dot{\varepsilon}_\theta}{dr} = \frac{\dot{\varepsilon}_r - \dot{\varepsilon}_\theta}{r}, \dots \dots \dots (3)$$

where  $\dot{\varepsilon}_r$  and  $\dot{\varepsilon}_\theta$  are the rates of change of strain in the radial and circumferential directions, respectively. The biaxial stress-strain rate law is [13]

$$\dot{\varepsilon}_\theta = k\bar{\tau}^{n-1} \left( \tau_\theta - \frac{1}{2}\tau_r \right), \dots \dots \dots (4)$$

$$\dot{\varepsilon}_r = B\bar{\tau}^{n-1} \left( \tau_r - \frac{1}{2}\tau_\theta \right), \dots \dots \dots (5)$$

where

$$\bar{\tau} = (\tau_r^2 - \tau_\theta^2 - \tau_r \cdot \tau_\theta)^{1/2} \dots \dots \dots (6)$$

To solve the problem for a disc with no central hole and supporting, say, no edge mass we must solve equations (1) – (6) simultaneously, subject to the boundary conditions

$$\tau_\theta = \tau_r \text{ at } r = 0, \dots \dots \dots (7)$$

$$\tau_r = 0 \text{ at } t = a \dots \dots \dots (8)$$

the simplest way of solving the equations seems to be to change the independent variable by making the substitution

$$x = \alpha r^2 \dots \dots \dots (9)$$

Equations (1) and (3) become, respectively:

$$\frac{d\tau_r}{dx} = \frac{\tau_\theta - \tau_r}{2x} - \frac{1}{2}, \dots \dots \dots (10)$$

$$\frac{d\dot{\varepsilon}_\theta}{dx} = \frac{\dot{\varepsilon}_r - \dot{\varepsilon}_\theta}{2x} \dots \dots \dots (11)$$

Differentiating equation (4) with respect to x, substituting for  $\frac{d\dot{\varepsilon}_\theta}{dx}$  from equation (11) and using equations (4) and (5) we have:

$$\frac{d\tau_\theta}{dx} \left[ 4 - 3(1 - m) \left( \frac{\tau_r}{\bar{\tau}} \right)^2 \right] = \frac{d\tau_r}{dx} \left[ 2(1 - 3m) - 3(1 - m) \left( \frac{\tau_r}{\bar{\tau}} \right) \left( \frac{\tau_\theta}{\bar{\tau}} \right) \right] - 3m, \dots \dots \dots (12)$$

where, as before,  $m=1/n$ .

Equations (12) and (10) make it possible to use a Runge - Kutta method to “march out” values of  $\tau_r$  and  $\tau_\theta$  for increasing x, if the value of  $\tau_r (= \tau_\theta)$  is known at  $x=0$ . We do not know the values of  $\tau_r$  and  $\tau_\theta$  at the origin, but we are free to assign a value, say,  $\tau_0$ , to them and apply a scale factor to all the stresses later on.

Equation (10) is determinate at  $x=0$ , but using L`Hopital`s rule we find

$$3 \frac{d\tau_r}{dx} - \frac{d\tau_\theta}{dx} = 1 \text{ at } x = 0 \dots \dots \dots (13)$$

Simultaneous solution of equations (12) and (13) at  $x=0$  gives the following starting derivatives at  $x=0$

$$\left. \begin{aligned} \frac{d\tau_r}{dx} &= -\frac{1}{4} \left( \frac{1+6m}{1+3m} \right) \\ \frac{d\tau_\theta}{dx} &= \frac{1}{4} \left( \frac{1-6m}{1+3m} \right) \end{aligned} \right\} \dots \dots \dots (14)$$

Fig. 2 shows the solutions, obtained by computer, for  $m=0$ ,  $m=0.4$  and  $m=1$ . It is easy to show that for  $m=1$   $d\tau_r/dx$  and  $d\tau_\theta/dx$  are independent of  $x$ . The radial stress becomes zero at  $x/\tau_0=16/7$ ; thus by equation (9), substituting for  $\alpha$ :

$$\tau_0 = 0.447 \left( \frac{\rho\omega^2 a^2}{g} \right).$$

It is readily checked that  $\bar{\tau}$  has a maximum at  $r=0$ .

For  $m=0$ ,  $\tau_r$  becomes zero at  $\frac{x}{\tau_0} = 3.25$ ; so far  $m=0$ ,  $\bar{\tau}_{max} = 0.308 \left( \frac{\rho\omega^2 a^2}{g} \right)$ . In this case, of course,  $\bar{\tau}$  is constant over the whole disc.

For discs supporting edge mass the boundary conditions are different. If the total mass, representing turbine blades, etc., is equal to  $\beta$  times the mass of the disc itself, and there is no circumferential cohesion in this mass, it is easily shown that at the rim, radius  $a$ ,

$$\tau_r = \frac{\beta\rho a^2 \omega^2}{2g} \dots \dots \dots (15)$$

A point such as A, Fig. 2, may represent the radial stress condition at the edge of the hole. Let the coordinates of A be

$$\frac{x}{\tau_0} = l, \quad \frac{\tau_r}{\tau_0} = k.$$

From equations (2) and (9):

$$\frac{\tau_0 g}{\rho a^2 \omega^2} = \frac{1}{l} \dots \dots \dots (16)$$

Combining equations (15) and (16) and substituting  $k = \tau_r/\tau_0$  we have

$$\beta = \frac{2k}{l}$$

Thus a line radiating from the origin as shown in Fig. 2 intersects the graphs of  $\frac{\tau_r}{\tau_0}$  for different values of  $m$  at values of  $x/\tau_0$  representing the edge of the plate for the same value of the parameter  $\beta$ .

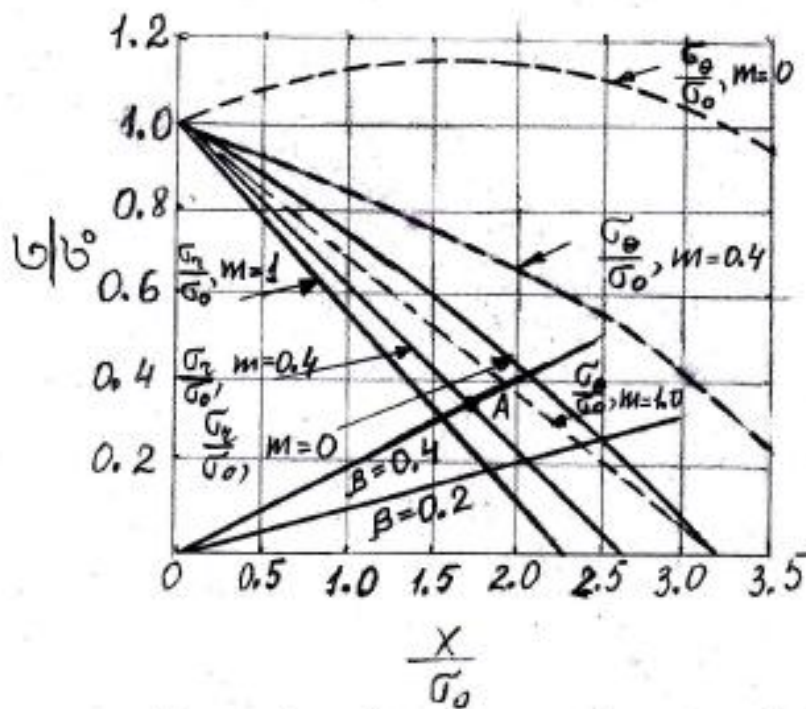


Fig. 2. Rotating disc solution

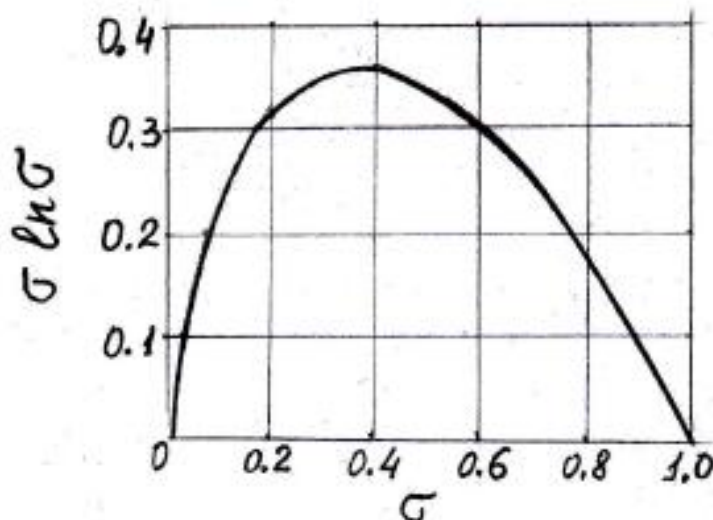


Fig. 3. Curve for use in "thermal" stress analysis

It should be noted that the solutions to this problem and similar problems presented in [17], sections 7-9, are not exact solutions, as implied in [17], but approximate “energy” solutions based on the deformed shape of linear-elastic plate [18].

the equilibrium equation at radius  $r$  is:

$$\frac{dM_r}{dr} = \frac{M_\theta - M_r}{r} - \frac{pr}{2}, \dots \dots \dots (17)$$

where  $M_r$  and  $M_\theta$  are the radial and circumferential bending moment per unit length and  $p$  is the uniformly distributed pressure.

The strain rate compatibility equation is

$$\frac{d\dot{k}_\theta}{dr} = \frac{\dot{k}_r - \dot{k}_\theta}{r}, \dots \dots \dots (18)$$

where  $\dot{k}_\theta$  and  $\dot{k}_r$  are the rates of change of curvature in the radial and circumferential directions respectively.

Using the “plane sections remain plane” conditions, it is easy to show (in the absence of membrane effects) that for a plate element of thickness  $H$

$$\dot{k}_r = G\bar{M}^{n-1} \left( M_r - \frac{1}{2}M_\theta \right), \dots \dots \dots (19)$$

$$\dot{k}_\theta = G\bar{M}^{n-1} \left( M_\theta - \frac{1}{2}M_r \right), \dots \dots \dots (20)$$

where

$$\left. \begin{aligned} \bar{M} &= \left( M_r^2 + M_\theta^2 - M_\theta M_r \right)^{\frac{1}{2}} \\ &\text{and} \\ G &= b \left( 1 + \frac{1}{2n} \right)^n \left( \frac{2}{H} \right)^{2n+1} \end{aligned} \right\} \dots \dots \dots (21)$$

Equations (17) – (20) are an exact analogue of equations (1) – (5) for the rotating disc. The quantities  $M_r, M_\theta, \dot{k}_r, \dot{k}_\theta$  correspond to  $\tau_r, \tau_\theta, \epsilon_r, \epsilon_\theta$  while  $p/2$  corresponds to  $\alpha$ . The boundary condition  $\tau_r = \tau_\theta$  at  $r=0$  also carries through. The equations may thus be solved in the same manner.

For the simply-supported plate the boundary condition  $M=0$  at the edge corresponds to the boundary condition for the rotating disc carrying no edge mass. For the clamped plate the relevant boundary condition at the edge is  $\dot{k}_\theta = 0$  or, using equation (20),  $M_r = 2M_\theta$ . The solutions (see Fig. 2) have to be marched out further to the point where this condition is satisfied. In the case  $n \rightarrow \infty$  there is a slight complication in that at the clamped boundary  $dM_r/dr \rightarrow \infty$ : this difficulty is easily overcome, however.

The greatest stress  $\bar{\tau}$  is readily found from the greatest value of  $\bar{M}$ . For the clamped plate, the greatest stress occurs at the edge, while for the simply-supported plate the greatest stress occurs at the centre – expect for the case  $n \rightarrow \infty$ , when the stress is equal to the yield stress everywhere.

E. Symmetrically stretched sheet with hole and ring reinforcement.

The results are taken from [16].

F. Thick – walled tube under internal pressure.

This problem was first solved by Bailey [19]. The analysis is much simplified by the fact that the strain rate in the axial direction is zero if the ends of the tube are closed. It is readily shown from the results (which are obtainable in [20]) that

$$\bar{\tau} = \frac{pm}{a^{-2m}-b^{-2m}} r^{-2m} \sqrt{3}, \dots \dots \dots (22)$$

where a and b are the internal and external radii, respectively. When m=0 the expression becomes indeterminate: L'Hospital's rule gives the perfectly plastic solution

$$\bar{\tau} = \frac{p\sqrt{3}}{2\ln\left(\frac{b}{a}\right)}$$

**Calculation of  $dF_m / dm$  at  $m=1$**

For any value of n for a given set of external loads we have a set of stresses  $\tau$  throughout the structure which are in equilibrium with the external loads, a set of strain rates  $\dot{\epsilon}$  which are compatible and which are related to the stresses by the material law

$$\dot{\epsilon} = B\tau^n \dots \dots \dots (23)$$

The stress distribution is identical to that which would be obtained for the same structure made of non-linear elastic material

$$\epsilon = B_1\tau^n \dots \dots \dots (23')$$

For the structure made of the analogous elastic material, consider a small change  $dn$  in n, and the associated changes in  $\epsilon$  and  $\tau$ . Differentiating equation (23') with respect to n:

$$\frac{d\epsilon}{dn} = (B_1n\tau^{n-1}) \frac{d\tau}{dn} + B_1\tau^n \ln\tau \dots \dots \dots (24)$$

In the special case n=1:

$$\frac{d\epsilon}{dn} = B_1 \frac{d\tau}{dn} + B_1\tau \ln\tau \dots \dots \dots (25)$$

Now  $\frac{d\epsilon}{dn}$  represents a compatible strain distribution, and  $\frac{d\tau}{dn}$  represents a stress distribution in equilibrium with zero external load. Equation (25) may thus be interpreted:  $\frac{d\epsilon}{dn}$  and  $\frac{d\tau}{dn}$  are changes in strain and stress in an initially unstressed linear-elastic structure (modulus of elasticity =  $1/B_1$ ) which is subject to a strain distribution (“thermal strain”) of  $B_1\tau \ln\tau$ .

Thus, if the stress distribution is known in the linear case,  $n=1$ , the rate of change of the stresses (and in particular of the greatest stress) with  $n$  may be determined from, essentially, a linear-elastic thermal stress problem. For  $n=1$ , of course,

$$\frac{d\tau}{dm} = -\frac{d\tau}{dn}$$

The result, as far as  $F_m$  is concerned, is independent of the magnitude of  $\tau$ . It is most convenient to scale the stresses so that in the greatest stress has absolute value unity. Fig. 3 shows a graph of  $\tau \ln \tau$  as a function of  $\tau$  for this case.

The analysis has been presented in terms of one-dimensional stress. The essential features carry through to triaxial stress systems. It should be noted that the “thermal” strains consist of changes in shape rather than changes in volume, as in conventional thermal stress analysis.

### References

- 1. Aret V. A., Eliseev A. M., Fedorova L. A.** Interpolation rule for estimating the greatest stress in a structure subject to creep. / Научный журнал НИУ ИТМО. Серия: процессы и аппараты пищевых производств. -№2-2013.-  
<http://processes.ihbt.ifmo.ru/file/article/7591.pdf>
- 2. Malivin N. N.** Applied theory of plasticity and creep. Moscow: “Mashinostroenie”, 1975.
- 3. Kachanov L. M.** Creep theory. Moscow: “Mashinostroenie”, 1973.
- 4. Mojarovsky N. C.** Theory of plasticity and creep in engineering. Kiev: “Vyshaja shkola”, 1991.
- 5. Kachanov L. M.** Applied theory of plasticity and creep. Moscow: “Mashinostroenie”, 1975.
- 6. Hoff, N. J.** Approximate analysis of structures in the presence of moderately large creep deformations. Q. Appl. Math. 1954, 12, 49.
- 7. Gubser, J. L. Sidebottow, O. M. and Shammamy, M. R.** Creep torsion in prismatic bars, joint International Conference on Creep, ASME, ASTM, I. Mech. E., 1963, Paper 54.
- 8. Hoff, N. J.** Buckling and stability, Wibur Wright Memorial Lecture, J. R. Aero. Soc., 1954, 58, 1.
- 9. Jonson, A. E.** Creep under complex stress systems at elevated temperature, Proc. Instn. mech. Engrs 1951, 164, 432.
- 10. Drucker, D. C. and Shield, R. T.** Bounds on minimum weight design, Q. Appl. Math., 1957, 15, 269.
- 11. Rabotnov Yu. N.** Creep rupture // Proceeding applied mechanics conference. Stanford University, 1968. P. 342-349.
- 12. Murakami S., Imazumi T.** Mechanical description. // J. mec. theor. et appl. 1982. Vol. 1 N5. P 743-761.
- 13. Hayhurt D. R.** Creep rupture under multi-axial states of stress. “Journal of the mechanics and physics of solids.” 1972. V.O. N6. P. 381-390.

**14. Jonson A. E.** Complex-stress creep of metals “Metallurgical Reviews. 1960. V.5. N20. P. 447-506.

**15. Rabotnov Yu. N.** Problems of mechanics of deformed solid. Moscow: Nauka, 1991.

**16. Fedorova L. A.** Disseptation II Inv. N33022, Research Institute “Gidropribor”, 1974.

**17. Finnie, I. and Heller, R. W.** Creep in engineering materials, 1959 (McGraw-Hill Book Co. Inc., New York).

**18. Malinin, N. N.** Continuous creep of round symmetrically loaded plates. Moscow: “Vysshe tekhn. u. trudy”. 1953. 26, 221.

**19. Bailey, R. W.** The utilization of creep test data in engineering design, Proc. Insin. mech. Engrs, 1935, 131.

**20. Nadai, A.** Theory of flow and fracture of solids, Vol. 1, 2<sup>nd</sup> ed., 1950 (McGraw-Hill Book Co. Inc., New York).